Genes & Diseases (2021) 8, 555–568

Available online at www.sciencedirect.com

ScienceDirect

journal homepage: http://ees.elsevier.com/gendis/default.asp

FULL LENGTH ARTICLE

The transcriptome of circulating cells indicates potential biomarkers and therapeutic targets in the course of hypertension-related myocardial infarction

Zilun Wei [a,1], Yining Yang [a,1], Qiaoling Li [b,1], Yong Yin [b,1], Zhonghai Wei [b,1], Wenfeng Zhang [a], Dan Mu [b], Jie Ni [b], Xuan Sun [b,**], Biao Xu [a,*]

[a] *Department of Cardiology, Nanjing Drum Tower Hospital, Clinical College of Nanjing Medical University, Nanjing, Jiangsu Province, 210008, PR China*
[b] *Department of Cardiology, Nanjing Drum Tower Hospital, Nanjing University Medical School, Nanjing, Jiangsu Province, 210008, PR China*

Received 9 October 2019; received in revised form 6 January 2020; accepted 8 January 2020
Available online 21 January 2020

KEYWORDS
Biological function;
Blood;
Hypertension;
Microarray;
Myocardial infarction;
Pathway

Abstract Hypertension (HT) is the most common public-health challenge and shows a high incidence around the world. Cardiovascular diseases are the leading cause of mortality and morbidity among the elderly (age > 65 years) in the United States. Now, there is widespread acceptance of the causal link between HT and acute myocardial infarction (MI). This is the first data-mining study to identify co-expressed differentially expressed genes (co-DEGs) between HT and MI (relative to normal control) and to uncover potential biomarkers and therapeutic targets of HT-related MI. In this manuscript, HT-specific DEGs and MI-specific DEGs and differentially expressed microRNAs (DE-miRNAs) were identified in Gene Expression Omnibus (GEO) datasets GSE24752, GSE60993, GSE62646, and GSE24548 after data consolidation and batch correction. Subsequently, enrichment in Gene Ontology (GO) terms and Kyoto Encyclopedia of Genes and Genomes (KEGG) pathways as well as protein–protein interaction networks were identified, and single-gene gene set enrichment analysis was performed to determine the affected biological categories and networks. Cross-matching of the results on co-DE-miRNAs and predicted miRNAs targeting the co-DEGs was conducted and discussed as well. We found that *MYC* and *HIST1H2BO* may

* Corresponding author. Department of Cardiology, Nanjing Drum Tower Hospital, Clinical College of Nanjing Medical University, Nanjing 210008, China
** Corresponding author. Department of Cardiology, Nanjing Drum Tower Hospital, Nanjing University Medical School, Nanjing 210008, China
E-mail addresses: sunxuan891119@163.com (X. Sun), xubiao62@nju.edu.cn (B. Xu).
Peer review under responsibility of Chongqing Medical University.
[1] Same contribution.

https://doi.org/10.1016/j.gendis.2020.01.007

be associated with HT, whereas *FCGR1A*, *FYN*, *KLRD1*, *KLRB1*, and *FOLR3* may be implicated in MI. Moreover, co-DEGs *FOLR3* and *NFE2* with predicted miRNAs and DE-miRNAs, especially miR-7 and miR-548, may be significantly associated and show huge potential as a new set of novel biomarkers and important molecular targets in the course of HT-related MI.

Introduction

Hypertension (HT) is by far the most common public-health problem with a high incidence around the world, regardless of ethnicity, sex, and geographic disparities.[1] It is the leading cause of premature death in advanced nations.[2] The residual lifetime risk for the middle-aged and elderly is 90%, indicating a huge public-health burden.[3] According to the anticipated changes in size and age composition, 29.2% of the world's population are predicted to have HT by 2025.[4] The rise is mainly due to drawbacks in preventive medicine and due to therapeutic inertia when blood pressure is uncontrolled. Thus, the burden of HT is now being transferred to low- and middle-income nations with backward disease surveillance and resources.[5] Recent studies linked HT pathogenesis with concomitant risks of cardiovascular, cerebrovascular, and kidney complications, particularly in the elderly.[6] In the United States, cardiovascular diseases (CVDs) are a serious complication in elderly individuals (age $>$ 65 years) and an important cause of mortality and morbidity.[1] Although mechanical complications of acute myocardial infarction (AMI) have been significantly reduced (to less than 1% of the cases) with new developments in pharmacotherapy, timely revascularization, and improved cardiac rehabilitation, the patients still face a poor prognosis, considering their worsened cardiac function and accelerated progression of heart failure after the operation.[7] An immune reaction and inflammatory response play critical roles in ischemic cardiac injury, in the postinfarction repair process, and in ischemia/reperfusion injury after temporarily enhanced blood flow following percutaneous coronary intervention, which is usually too late for a risk assessment.[8] Validated cardiac biomarkers such as BNP and CRP provide only limited information about what is already known or being measured.[9] In contrast, primary prevention of CVD depends mostly on the capacity to recognize at-risk individuals long before AMI. Novel molecular markers for early detection and continuous monitoring might help researchers to reveal initial dysregulation and the underlying mechanisms and will guide healthcare professionals to ensure formulation of the correct therapeutic regimen.

HT has grown in prevalence, and today, HT is widely accepted to be causally linked with AMI in the general population. Although CVD-related mortality does not increase along with any increases within the normal range of blood pressure, each additional 20 mmHg of systolic blood pressure or 10 mmHg of diastolic blood pressure leads to more than a 2-fold increase in the rate of death from ischemic heart disease in the age group "40–69 years." With age, the annual absolute risk of HT-related CVDs, especially ischemic heart disease and AMI, increases exponentially.[10] HT is usually a predictor of serious physical illnesses and even death in the early post-AMI period. Lowering of high blood pressure correlates with a lessened CVD burden,[11] but the actual risk of major adverse cardiovascular events or all-cause deaths during a follow-up period as long as 330 days is not associated with a history of HT probably because timely recanalization and medication compliance might alleviate the adverse influences of prior HT.[12] There is an inconsistent relation between blood pressure elevation recorded after stabilization of hemodynamics following acute ischemic events and repeated coronary events during long-term follow-up, whereas lower systolic blood pressure during chest pain episodes is always linked with lower mortality within 1 year from stenosis or occlusion of large vessels.[13] According to the above-mentioned complex relation, the absolute value of blood pressure might not perfectly reflect the onset and development of myocardial infarction (MI); therefore, researchers thinking outside the box and exploring the integrated molecular mechanisms might broaden the understanding of HT-related MI from a different perspective.

As an emerging technology for characterizing the landscape of differentially expressed genes (DEGs), differentially expressed proteins, and differentially produced metabolites in the course of CVD, microarray gene expression data provide a comprehensive perspective on pathological mechanisms by integrating the data on dysregulated pathways and possible interactions. To compensate the shortage of tissue-based microarray profiles, particularly those of the human heart and cardiac vessels, Liew et al have compared the complexity of the blood transcriptome with gene expression levels in 9 organs of the human body.[14] The results showed that expression levels of over 80% genes were consistent between any given tissue and blood, suggesting that peripheral blood is an ideal surrogate tissue to discover genes and pathways that play important roles in the pathogenesis and progression of such diseases. We herein conducted a peripheral-blood whole-genome microarray transcriptional analysis based on public datasets in a prospective cohort of patients with AMI by means of cross-platform integration to improve reproducibility and robustness of gene signature biomarkers. This is the first data-mining study to identify coexpressed differentially expressed genes (co-DEGs) of HT and MI and to elucidate the molecular mechanisms and pathophysiology by means of HT-specific DEGs (HT-DEGs) and MI-specific DEGs (MI-DEGs). Gene set enrichment analysis (GSEA) was performed on the co-DEGs for pathway analysis. At the end of this paper, we demonstrate potential microRNAs (miRNAs; by studying overlaps of gene sets) specific for HT patients susceptible to MI.

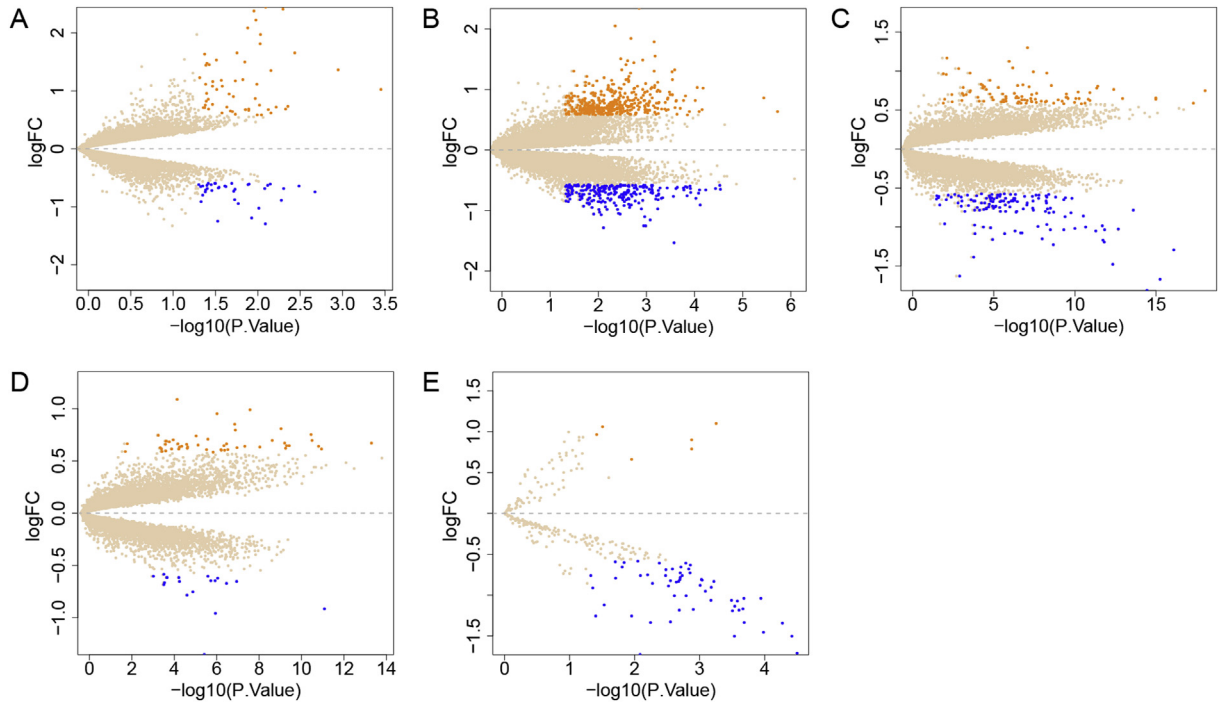

Figure 1 The volcano plot of the microarray mRNA or miRNA expression in GEO datasets. (**A**) The volcano plot of mRNA profile GSE-HT (GSE24752). (**B—D**) The volcano plot of mRNA profile GSE-MI (GSE60993 and GSE62646 separately and combined data of GSE60993 and GSE62646 after batch correction). (**E**) The volcano plot of miRNA profile mi-GSE-MI (GSE24548). Orange: higher expression, blue: lower expression.

Results

Identification of HT-DEGs and MI-DEGs

A total of 14,973 probes were identified, which were consistent with 46,674 genes in GSE-MI (GSE60993 and GSE62646) after the batch correction. Almost 10,001 probe sets were selected for the 22,283 genes of GSE-MI and GSE-HT (GSE24752), and MI-DEGs and HT-DEGs were confirmed. Patients with HT-complications, like diabetes, smoking, renal failure, coronary artery disease (CAD), stroke, peripheral artery disease (PAD), were not included. We found 70 DEGs in blood samples from patients that underwent emergency percutaneous coronary intervention as compared to control patients within 24 h of hospitalization, and we designated 93 DEGs as the HT-DEGs in hypertension patients. The volcano plot of DEG inclusion criteria is given in Fig. 1. Heatmaps of MI-DEGs in terms of an immune response, cellular signaling, and an inflammatory response were constructed for analysis of gene expression, and these data are displayed in Fig. 2A—C. Fig. 2D—F shows the gene expression values corresponding to an immune response, cell signaling, and T-cell activation among the above HT-DEGs.

Construction of interaction networks and functional enrichment evaluation

We identified 58 and 44 nodes in the PPI networks of MI-DEGs and HT-DEGs, respectively, and these data are presented in Fig. 3. Here, hub nodes (proteins) called high-affinity immunoglobulin γ Fc receptor I (FCGR1A; the degree of intranode connectivity (degree) = 14), a tyrosine protein kinase (FYN; degree = 13), transcription factor PU.1 (SPI1; degree = 12), natural killer cell antigen CD94 (KLRD1; degree = 10), HLA class I histocompatibility antigen α chain E (HLA-E; degree = 9), cytidine deaminase (CDA; degree = 8), killer cell lectinlike receptor subfamily B member 1 (KLRB1; degree = 7), actin-related protein 2 (ACTR2; degree = 6), and folate receptor γ (FOLR3; degree = 5) were detected among MI-DEGs because of the relatively higher degree. However, the genes including regulatory subunits of the 26S proteasome non-ATPase (*PSMA*, *PSMB*, *PSMC*, and *PSMD*; degree = 20—22) and Myc proto-oncogene (*MYC*; degree = 9) were regarded as hub genes in relation to HT maintenance.

In the DAVID database, the top 5 GO terms (biological processes) related to HT-DEGs were found to be primarily associated with amino acid transport (*p* value: 1.37E—06), positive regulation of interferon-gamma production (*p* value: 0.01), T cell receptor signaling pathway (*p* value: 0.02), interferon-gamma-mediated signaling pathway (*p* value: 0.03), and T cell costimulation (*p* value: 0.03). Among cellular components, there was a significant correlation with the MHC class II protein complex (*p* value: 0.07) and the integral component of lumenal side of endoplasmic reticulum membrane (*p* value: 0.09). In addition, the enriched GO terms from the category "molecular functions" were MHC class II receptor activity (*p* value: 0.04) and protein heterodimerization activity (*p* value: 0.05). With respect to MI-DEGs, the following biological processes (GO terms) were significantly enriched: defense response (*p*

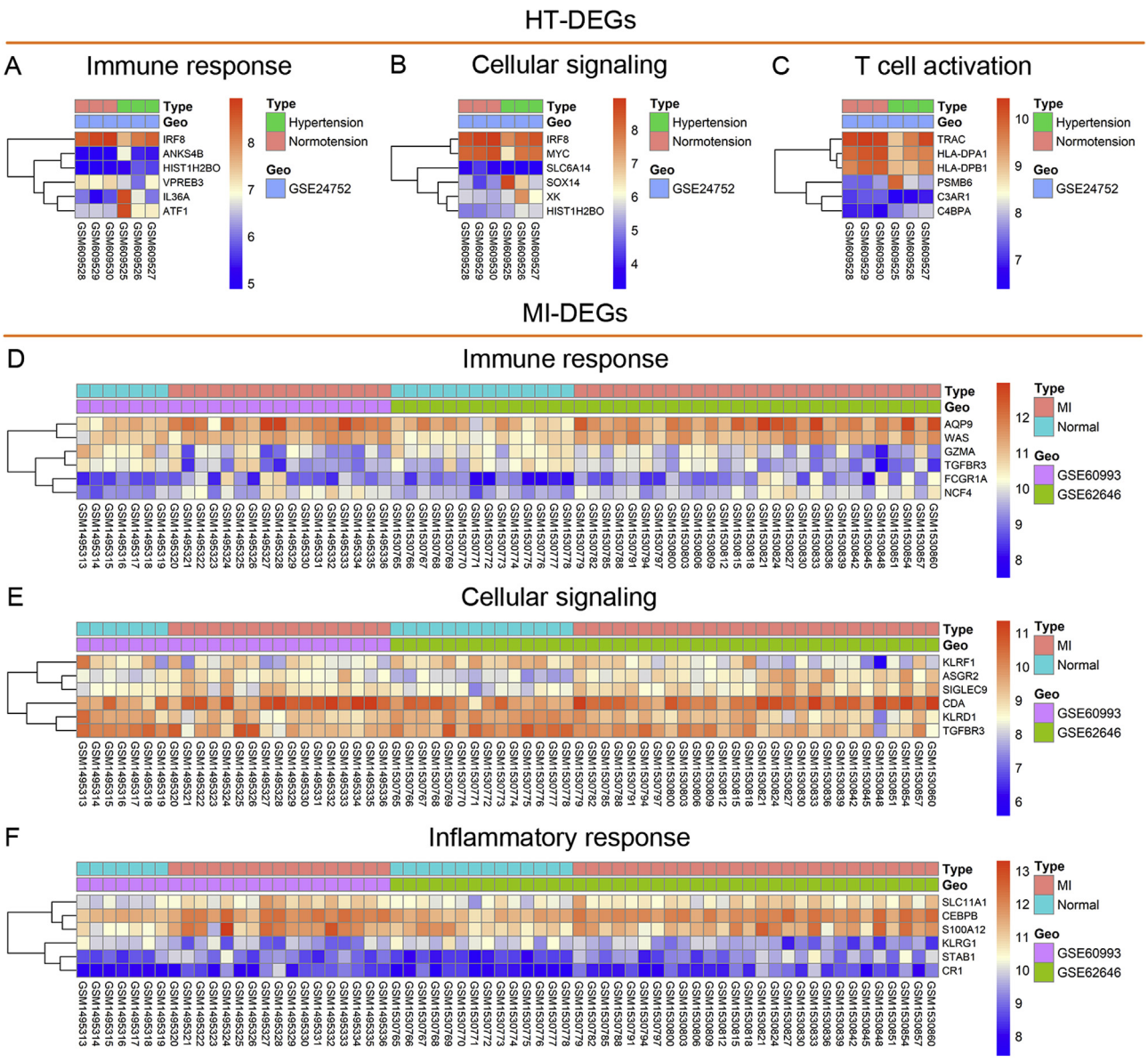

Figure 2 Hierarchical clustering analysis of DEGs. (**A**—**C**) Results of hierarchical clustering analysis of expression of HT-DEGs in relation to immune responses, cellular signaling, and T-cell activation. (**D**—**F**) Results from hierarchical clustering analysis of expression of MI-DEGs in relation to immune responses, cellular signaling, and an inflammatory response. Orange: higher expression, blue: lower expression.

value: 4.00E-06), immune response (*p* value: 1.19E-04), cell surface receptor signaling pathway (*p* value: 4.27E-04), natural killer cell mediated immunity (*p* value: 7.13E-03), inflammatory response (*p* value: 0.05), and positive regulation of angiogenesis (*p* value: 0.06). Among cellular components, there was enrichment of extracellular region (*p* value: 3.04E-04), integral component of membrane (*p* value: 0.02), and integral component of plasma membrane (*p* value: 0.02). The following molecular functions (GO terms) were found to be enriched: carbohydrate binding (*p* value: 4.37E-07), transmembrane signaling receptor activity (*p* value: 7.04E-03), receptor activity (*p* value: 7.38E-03), MHC class I protein complex binding (*p* value: 0.01), serine-type endopeptidase activity (*p* value: 0.01), and protein antigen binding (*p* value: 0.02; Fig. 4A and B).

KEGG pathway analysis results are illustrated in Fig. 4C, D. The results suggested that the set of HT-DEGs was mainly enriched in multiple pathways of inflammatory diseases, including systemic lupus erythematosus (*p* value: 2.20E-03), complement and coagulation cascades (*p* value: 4.30E-03), TGF-β signaling pathway (*p* value: 7.00E-03), allograft rejection (*p* value: 0.01), graft-versus-host disease (*p* value: 0.01), type 1 diabetes mellitus (*p* value: 0.01), autoimmune thyroid disease (*p* value: 0.02), inflammatory bowel disease (*p* value: 0.03), antigen processing and presentation (*p* value: 0.04), and Th1 and Th2 cell differentiation (*p* value: 0.05). In the set of MI-DEGs, inflammatory and immune-system-related KEGG terms were found to be enriched, including antigen processing and presentation (*p* value: 3.97E-04), natural killer cell

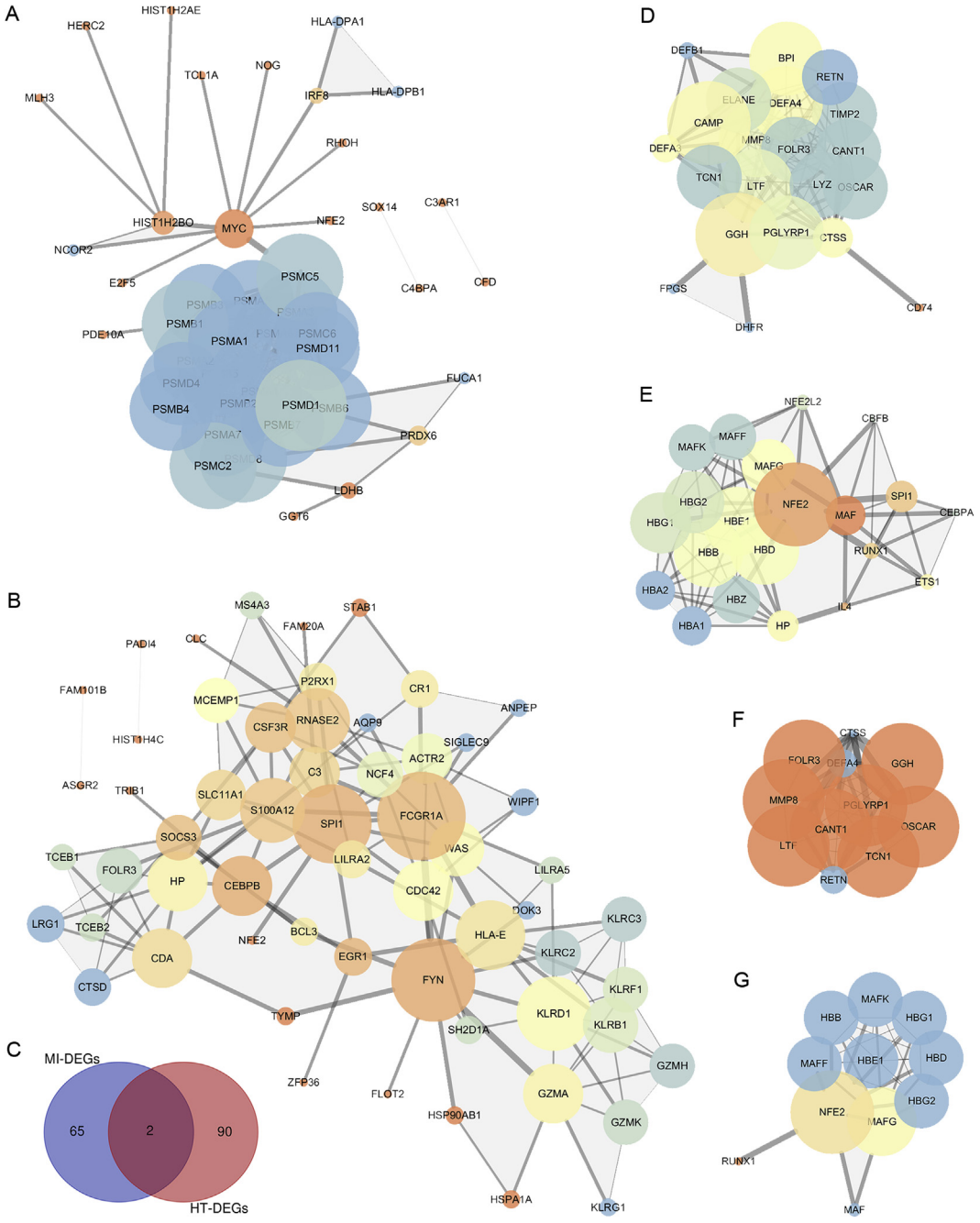

Figure 3 PPI network and Venn diagrams: **(A-B)** PPI networks according to the STRING database for HT-DEGs and MI-DEGs, respectively (threshold $>$ 0.4). **(C)** Venn diagrams of co-DEGs specific to HT-related MI. Two co-DEGs, *FOLR3* and *NFE2*, were identified. **(D—G)** PPI networks according to the STRING database for the module including *FOLR3* and *NFE2* among HT-DEG and MI-DEGs, respectively (threshold $>$ 0.4). Nodes: proteins, interactions (edges): lines between DEGs.

mediated cytotoxicity (*p* value: 2.89E-03), tuberculosis (*p* value: 8.71E-03), TNF signaling pathway (*p* value: 0.01), acute myeloid leukemia (*p* value: 0.04), adipocytokine signaling pathway (*p* value: 0.04), and PPAR signaling pathway (*p* value: 0.04; Fig. 4 C and D).

Analysis of enrichment with GO terms using the REACTOME database uncovered additional associations as confirmation and supplementary information. The HT-DEG set turned out to be enriched in such terms as complement cascade (*p* value: 1.07E-03), transcription of E2F targets under negative control by DREAM complex (*p* value: 1.97E-03), translocation of ZAP-70 to immunological synapse (*p* value: 1.97E-03), phosphorylation of CD3 and TCR zeta chains (*p* value: 2.64E-03), PD-1 signaling (*p* value: 2.89E-03), interferon gamma signaling (*p* value: 4.01E-03), "RUNX1 regulates genes involved in megakaryocyte differentiation and platelet function" (*p* value: 4.66E-03), downstream TCR signaling (*p* value: 4.79E-03), signaling by TGF-beta family members (*p* value: 5.36E-03), and TCF dependent signaling in response to WNT (*p* value: 8.61E-

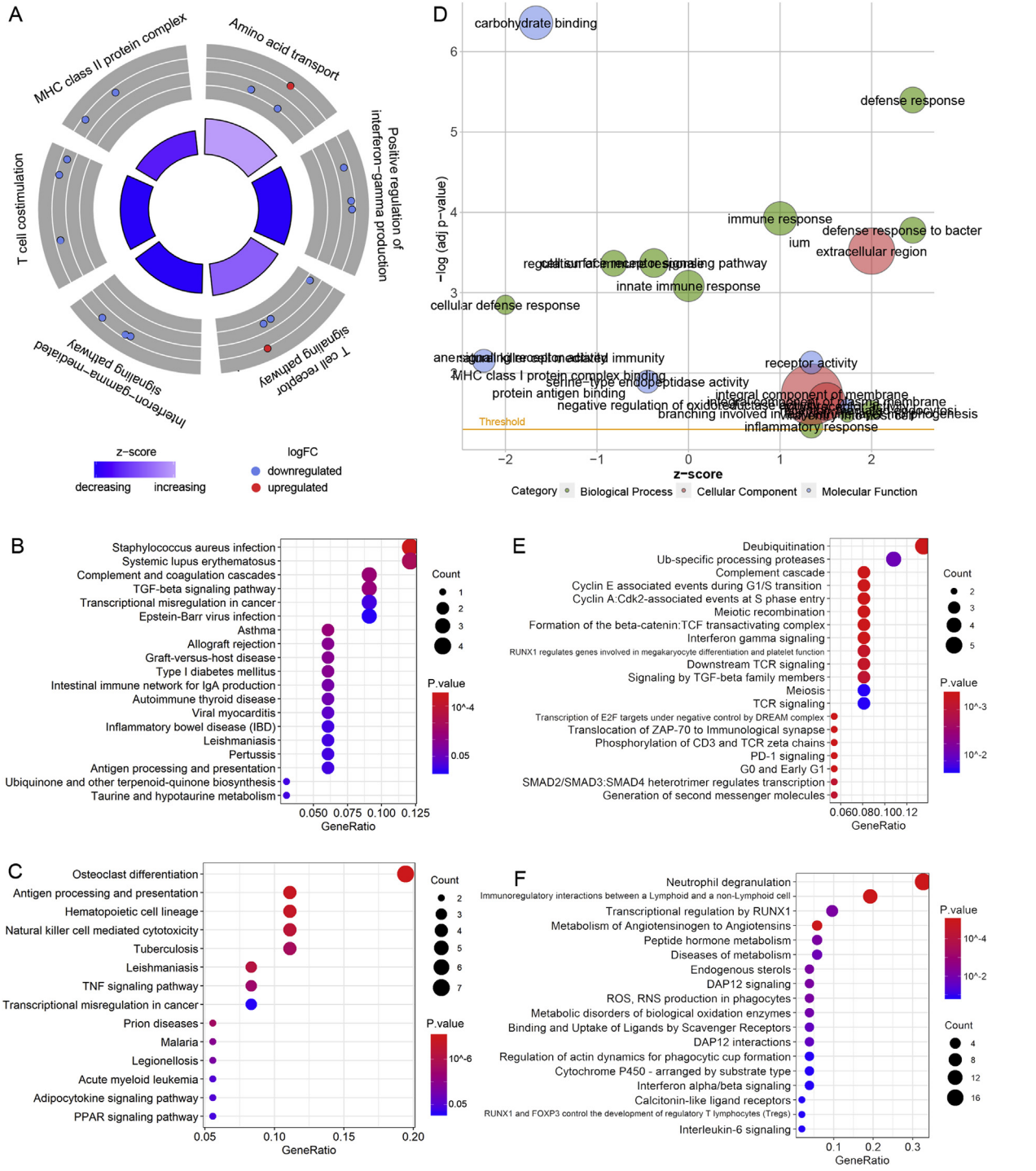

Figure 4 Dot plots of enrichment in GO terms and KEGG pathways: **(A** and **D)** GO term enrichment of the HT-related DEG set and MI-related DEG set, respectively. **(B** and **E)** KEGG pathway enrichment of the HT- and MI-related DEG sets, respectively. **(C** and **F)** Functional and pathway enrichment according to the Reactome database for the HT- and MI-related DEG sets, respectively. Dot sizes represent counts of enriched DEGs, and dot colors represent negative $\log_{10}$P values. Red: higher expression, blue: lower expression.

03). Similar results were obtained for MI-DEGs, including neutrophil degranulation (*p* value: 5.53E-11), immunoregulatory interactions between a lymphoid and a non-lymphoid cell (*p* value: 6.69E-10), metabolism of angiotensinogen to angiotensins (*p* value: 7.29E-05), endogenous sterols (*p* value: 7.71E-03), peptide hormone metabolism (*p* value: 9.50E-03), ROS, RNS production in phagocytes (*p* value: 0.01), metabolic disorders of biological oxidation enzymes (*p* value: 0.01), interferon alpha/beta signaling (*p* value: 0.05), "RUNX1 and FOXP3 control the development of regulatory T lymphocytes" (*p* value: 0.05), and interleukin-6 signaling (Fig. 4E and F).

Table 1 Cardiovascular disease portal and gene ontology annotation overview of human species and human synteny.

Disease	Category	Term	genes
Hypertension (755 total genes)	GO (Cellular Component)	Cell	977
		Plasma membrane	693
		Cytoplasm	452
		Nucleus	348
		Extracellular region	265
	GO (Biological Process)	Multicellular organism development	2k
		Signal transduction	1k
		Response to stress	762
		Anatomical structure morphogenesis	593
		Cell differentiation	530
		Cell death	505
	GO (Molecular Function)	Protein binding	1k
		Receptor activity	523
		Catalytic activity	472
		Signaling receptor binding	347
		Hydrolase activity	265
		Nucleotide binding	227
MI (339 total genes)	GO (Cellular Component)	Cell	408
		Plasma membrane	368
		Cytoplasm	270
		Extracellular space	187
		Nucleus	187
	GO (Biological Process)	Multicellular organism development	836
		Response to stress	536
		Signal transduction	470
		Anatomical structure morphogenesis	370
		Cell death	363
		Cell differentiation	295
	GO (Molecular Function)	Protein binding	842
		Catalytic activity	237
		Receptor activity	201
		Signaling receptor binding	200
		Peptidase activity	145
		Nucleotide binding	93

https://rgd.mcw.edu.

Biological-category enrichment and disease-related prediction scores for the co-DEGs

The Rat Genome Database (RGD, http://rgd.mcw.edu) is a valuable resource with a large amount of rat and human genetic data and resources, such as information on genes, quantitative trait loci, microsatellite markers, and rat strains. After recent system updates, the RGD can serve as a high-quality human-disease-centric resource based on emerging *H. sapiens* genomic sequence and annotation pipelines.[15] By digging into disease-related connections between HT and MI, we found a high degree of overlap in the biological functions between the HT-specific and MI-specific gene sets. Proteins encoded by the related gene sets are located mostly on the plasma membrane. The progression of diseases was found to significantly affect some biological processes, such as multicellular organism development, signal transduction, and response to stress. The changes in cellular function mentioned above are mainly caused by changes in protein binding, catalytic activity, and receptor activity at the molecular level (Table 1). Although detailed molecular targets and pathways during disease onset and development were not specifically identified, these data are remarkably similar to our results on biological-category enrichment in datasets GSE24752, GSE60993, and GSE62646 (as depicted in Fig. 2 and 4).

To generate gene—disease annotations in detail and to gain a deeper understanding of the genetic changes that are identical between HT patients and MI patients, the Venn map was constructed, and the co-DEGs between HT-DEGs and HT-DEGs were identified (Fig. 3C and Table 2). Of note, only 2 co-DEGs were found. The expression of *FOLR3* and *NFE2* was low in patients with HT (log_2FC: −1.03, P value: 9.76E-03, and log_2FC: −0.75, P value: 0.04, respectively), and just the opposite happened soon after AMI (log_2FC: 0.66, *p* value: 0.02, and log_2FC: −0.64, *p* value: 4.58E-07, respectively). In a comparison between HT and MI, the PPI network showed similar proteins interacting with FOLR3, and the same was true for NFE2, thus indicating possible similarity of upstream and downstream interactions and biological functions between the 2 diseases (Fig. 3D—G). The Comparative Toxicogenomics Database

Table 2 Venn diagrams of DEGs of hypertension patients (HT-DEGs) and myocardial infarction patients (MI-DEGs).

Terms	Total	Elements
MI-DEGs	65	STAB1, FLOT2, KCTD12, DOK3, CYP27A1, NCF4, S100A12, ASGR2, TRIB1, ZFP36, LILRA2, GZMH, CTSD, TGFBR3, CEBPB, KLRC3, AQP9, RNASE2, LOC441081, FAM20A, ACSL1, SOCS3, SH2D1A, HIST1H4C, TCN2, CDA, CSF3R, SAMD3, ZNF467, FAM101B, LRG1, SLC11A1, ADM, TARP, SDAD1, SIGLEC9, LILRA5, FCGR1A, MCOLN2, CLC, LILRA3, TBC1D2, KLRD1, ANPEP, SPI1, GZMA, PADI4, CYP1B1, EGR1, P2RX1, DYSF, MCEMP1, GZMK, C1orf21, BCL3, MLF2, CR1, KLRB1, KLRC2, MS4A3, KLRG1, WAS, KLRF1, HP, HSPA1A
HT-DEGs	90	ZDHHC14, NKAPP1, ACIN1, PVRIG, LINC00473, FAM186B, LOC102724275, C4BPA, SLC4A1, LOC101928893, ZNF891, COQ3, PSMB6, TMEM43, PLA1A, C3AR1, LINC00689, HLA-DPB1, MLH3, HOTAIRM1, E2F5, IL36A, LOC100506922, RP11-395I6.3, RP11-466A19.8, OR2L13, HIP1, DTHD1, LMTK3, RP11-554J4.1, KCNV1, ACP1, HLA-DPA1, XK, LINC00403, HIST1H2BO, MYC, ANKS4B, C10orf126, RHOH, VPREB3, LDHB, SPEF1, WFDC6, NOG, GGT6, RBMS3-AS3, ND6, OTUB2, HHEX, LOC285556, LOC643085, ERICH4, CSN1S2AP, PLEKHF2, PRDX6, FAM32A, ATF1, HERC2, SLC6A14, POU6F2-AS2, FAM170A, RP11-184E9.2, TMEM55A, RP6-99M1.2, AKNAD1, FUCA1, SOX14, CELF2-AS1, TMIE, CFD, RP11-843B15.2, C17orf98, TRAC, LINC00551, LOC100507537, CTC-510F12.4, PCTP, AX747191, IRF8, VWA5A, CTBP1-AS, LOC100506563, TCL1A, RP11-568N6.1, ZNF385B, CHRM3-AS2, HIST1H2AE, MAGEB6, SKAP2
Overlapped DEGs	2	NFE2, FOLR3

showed that the co-DEGs were associated with several CVDs and metabolic diseases, and these data are presented in Fig. 5. Given that the functional enrichment mentioned earlier was observed in a group of genes with significantly altered expression, we used the GSEA of the GEO datasets to explore the potential functions of FOLR3 and NFE2. Because the metric that we selected for ranking gene parameters (Signal2Noise or tTest) requires at least 3 samples for each phenotype, GSE24752 (the HT dataset) failed GSEA owing to too few samples ($n = 1$ for HT and $n = 2$ for control) for both phenotypes. For MI analysis, we divided the expression profiling data into datasets "*FOLR3* (or *NFE2*) lower expression" and "*FOLR3* (or *NFE2*) higher expression" according to the median FOLR3 (or NFE2) expression level in the batch-corrected MI dataset (combined datasets GSE60993 and GSE62646) after removal of the control data. Comparison of transcript levels between the *FOLR3* (or *NFE2*) higher expression and lower expression groups of blood samples from patients with MI revealed a number of DEGs. Our results showed that both FOLR3 and NFE2 expression significantly upregulated autophagy pathways and downregulated pathways related to energy metabolism, including alanine, aspartate, and glutamate metabolism; butanoate metabolism; the citrate cycle; the tricarboxylic acid (TCA) cycle; glycolysis; gluconeogenesis; and pyruvate metabolism (Fig. 6 and Table 3). Collectively, GO term and KEGG pathway enrichment analyses and GSEA of datasets GSE60993 and GSE62646 indicated that the low expression of *FOLR3* and *NFE2* affects the activity of cellular metabolism and influences autophagy and cell

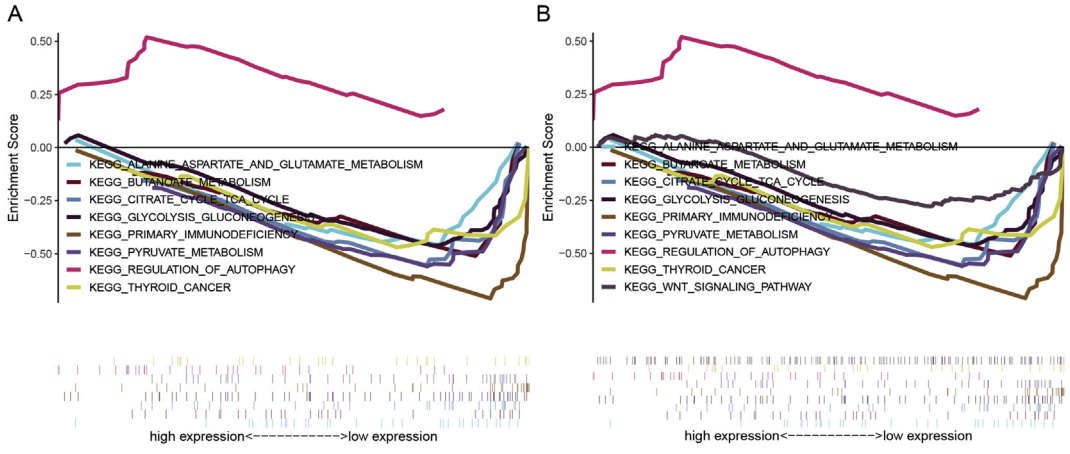

Figure 5 GSEA of expression of co-DEGs in patients with MI. (**A**) Expression profiling data were divided into datasets "NFE2 lower expression" and "NFE2 higher expression" according to the median NFE2 expression level. (**B**) Expression profiling data were divided into datasets "FOLR3 lower expression" and "FOLR3 higher expression" according to the median FOLR3 expression level in the batch-corrected MI dataset (combined datasets GSE60993 and GSE62646). Visualization was implemented in GSEA 3.0 software. The final map was generated by means of R packages "plyr," "ggplot2," "grid," and "gridExtra" for removal of any general or noninformative smaller networks to simplify the final diagram.

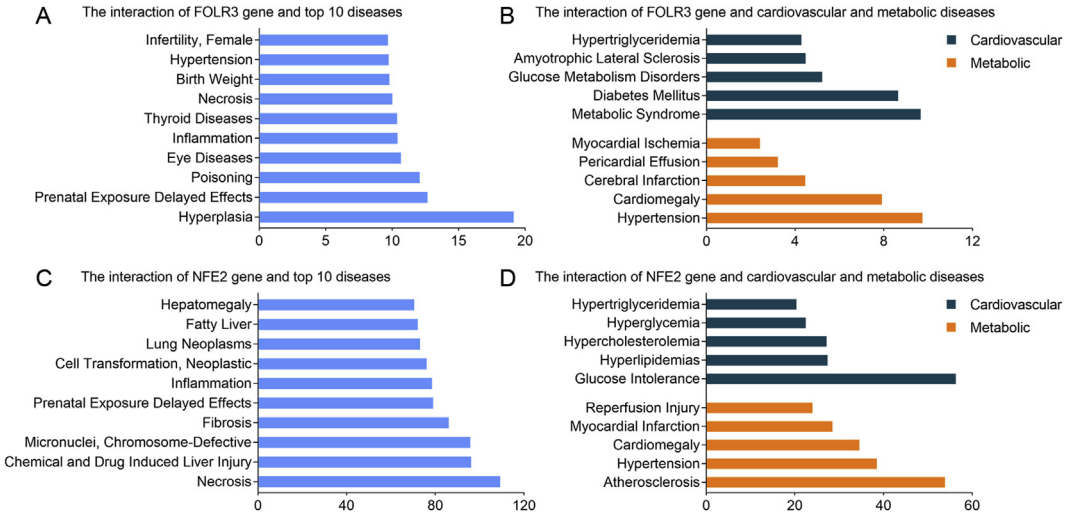

Figure 6 Relations with various diseases in general, metabolic diseases in particular, and CVDs related to the co-DEGs according to the Comparative Toxicogenomics Database. (**A-B**) Results from the Comparative Toxicogenomics Database on NFE2. (**C-D**) Results from the Comparative Toxicogenomics Database on FOLR3.

death, thereby contributing to changes in the overall expression level of genes after aggressive AMI.

Prediction of miRNAs targeting co-DEGs and analysis of the actual expression levels

Table 4 shows the top 5 carefully predicted miRNAs targeting each co-DEG involved in HT-related MI as a result of combined application of mirDIP, miRWalk, and TargetScan tools. These data gave us an ingenious way to understand how predicted miRNAs correlate with the progression of HT-related MI. GSE24548 contains a miRNA expression profile of platelet samples from 4 patients with their very first AMI and from 3 controls. By modulating the predicted miRNAs and differentially expressed miRNAs (DE-miRNAs) after MI, we hope to determine a more realistic miRNA—mRNA network around key miRNAs (hsa-miR-7-5p, log_2FC: −0.82, P value: 2.80E-03, and hsa-miR-548-5p, log_2FC: −1.05, P value: 1.14E-04) during MI (Fig. 7).

Discussion

Detecting HT is necessary to prevent AMI. However, inadequate blood pressure monitoring, medication noncompliance, an unhealthy lifestyle, and poor sensitivity to blood pressure fluctuations in the elderly limit effective target control and even cause HT emergencies.[4,5,16] Identification of markers and associations between HT and MI is therefore worthy of attention and may reveal a target for primary prevention and community therapy. In this study, biological functions such as the inflammatory and immune response,

Table 3 GSEA enrichment results for FOLR3 and NEF2C genes with original data obtained from GSE60993 和 GSE62646.

Gene	Regulation	Term	ES	NES	P value
FOLR3	Up	KEGG_REGULATION_OF_AUTOPHAGY	0.5199144	1.668857	0.008180
	Down	KEGG_PYRUVATE_METABOLISM	−0.58483	−1.67831	0.010395
		KEGG_BUTANOATE_METABOLISM	−0.57011	−1.67309	0.010309
		KEGG_ALANINE_ASPARTATE_AND_GLUTAMATE_METABOLISM	−0.50376	−1.66442	0.002066
		KEGG_GLYCOLYSIS_GLUCONEOGENESIS	−0.4773	−1.65101	0.017647
		KEGG_PRIMARY_IMMUNODEFICIENCY	−0.73625	−1.59229	0.012605
		KEGG_THYROID_CANCER	−0.49717	−1.5756	0.047325
		KEGG_CITRATE_CYCLE_TCA_CYCLE	−0.5862	−1.54846	0.069106
NFE2C	Up	KEGG_REGULATION_OF_AUTOPHAGY	0.519914	1.695634	0.012000
		KEGG_PYRUVATE_METABOLISM	−0.58483	−1.75248	0.012121
		KEGG_BUTANOATE_METABOLISM	−0.57011	−1.72362	0.010204
		KEGG_ALANINE_ASPARTATE_AND_GLUTAMATE_METABOLISM	−0.50376	−1.70064	0.009921
		KEGG_PRIMARY_IMMUNODEFICIENCY	−0.73625	−1.64576	0.005769
		KEGG_GLYCOLYSIS_GLUCONEOGENESIS	−0.4773	−1.61349	0.009843
		KEGG_CITRATE_CYCLE_TCA_CYCLE	−0.5862	−1.58633	0.062124
		KEGG_THYROID_CANCER	−0.49717	−1.56898	0.039293
		KEGG_WNT_SIGNALING_PATHWAY			0.062500

Table 4 The Gene Ontology (GO) terms and Kyoto Encyclopedia of Genes and Genomes (KEGG) pathways enrichment among predicted miRNAs and Co-DEGs.

Genes	Predicted miRNAs	Category	Term	genes	miRNAs	P value
FOLR3	hsa-miR-7-5p	KEGG	Fatty acid biosynthesis	4	2	2.42e-19
	hsa-miR-548-5p		Hippo signaling pathway	46	5	6.31e-06
	hsa-miR-6077		Adherens junction	29	5	1.92e-04
	hsa-miR-876-5p		Estrogen signaling pathway	21	5	2.66e-03
	hsa-miR-1290		Protein processing in endoplasmic reticulum	18	5	1.77 e-03
		GO	Cellular nitrogen compound metabolic process	880	5	1.58e-173
			Ion binding	994	5	2.62e-88
			Response to stress	396	5	3.33e-23
			Epidermal growth factor receptor signaling pathway	57	5	1.97e-14
			Fibroblast growth factor receptor signaling pathway	52	5	5.82e-12
NFE2	hsa-miR-146b-5p	KEGG	Cocaine addiction	14	4	5.22e-04
	hsa-miR-2115-3p		Thyroid hormone synthesis	16	3	1.40e-03
	hsa-miR-518f-5p		ErbB signaling pathway	25	4	1.86e-03
	hsa-miR-7515		Circadian rhythm	11	3	0.029
	hsa-miR-329-3p		Vasopressin-regulated water reabsorption	15	4	0.043
		GO	Cellular nitrogen compound metabolic process	648	5	5.19e-83
			Ion binding	770	5	4.70e-48
			Response to stress	297	5	1.12e-12
			Protein binding transcription factor activity	79	5	7.14e-10
			Epidermal growth factor receptor signaling pathway	42	5	6.71e-09

cellular signaling as well as T-cell activation and development were found to be closely related to the maintenance and onset of HT and to AMI through combined mining of public databases. A few hub genes—directly or indirectly coregulating the endocrine and cardiovascular systems—were found among the HT-DEGs through Comparative Toxicogenomics Database-mediated prediction of the PPI network and diseases. For example, a distinctive feature of HT in the heart is hypertrophy, meaning limited capacity for adaptation. This age-related mechanical load in the myocardium is mainly due to diminished induction of proto-oncogene *MYC* on the molecular level.[17] Increased MYC expression is observed in hypertrophied hearts, whereas a heart-specific knockdown of *MYC* expression postpones and reverses the progression of cold-induced cardiac hypertrophy with decreased cardiac output, left ventricle wall thickness, and decreased heart weight.[18] HIST1H2BO is a core histone among the proteins wrapped around DNA and forms the nucleosome structure of the chromosomal fiber. Changes in HIST1H2BO expression are seen in differentiated macrophages and systemic lupus erythematosus, an autoimmune disease induced by prolonged exposure of apoptotic cells to the immune system.[19] Dysregulation of HIST1H2BO expression is accompanied by abnormal inflammatory infiltration, and the causes of this dysregulation in HT are yet to be studied. Cardiac troponins, CK-MB, total CK, and myoglobin are already widely used as key diagnostic and prognostic markers in clinical practice. We also found several candidate marker genes whose expression changed significantly in blood samples from patients with MI as early as within 4 h of admission. Short-type peptidoglycan recognition protein 1 gene (*PGLYRP1*) encodes an innate-immunity protein that directly breaks down the structure of microbial cell wall peptidoglycan (PGNs) and plays an important part both in antibacterial defenses and several inflammatory diseases.[20,21] FYN-dependent phosphorylation of a nonreceptor protein tyrosine kinase activates immunoreceptor signaling. FYN deficiency is protective, whereas FYN activation is detected in patients with lupus nephritis, a severe complication of systemic lupus erythematosus.[22] The SPI1 transcription factor has been proven to be a key modulator of hematopoiesis processes and inhibits the self-renewal function of hematopoietic stem cells,[23] whereas human leukocyte antigen E (HLA-E), a nonclassical major histocompatibility complex class I molecule, has been identified as a marker of hematological cancers at terminal stages.[24]

Additionally, research attention should be focused on *FOLR3* and *NFE2*: the 2 co-DEGs of HT and MI. A loss of function or variants of folate receptor FOLR3 may affect folate availability, and folic acid has been reported to reduce serum homocysteine levels and (in some cases) blood pressure. Hyperhomocysteinemia above the normal range (5—15 μmol/L) has been identified as an independent predictor of CVDs and HT, in addition to reducing the integrity of vascular endothelial cells and smooth muscle cells that maintain the integrity of blood vessels as well as renal function.[25,26] Elevated homocysteine levels induce a hypercoagulation state, makes a clot more resistant to fibrinolysis, and contributes to inflammation and oxidative stress: the 2 key mechanisms underlying the pathological changes during CVD.[27,28] Earlier studies suggest that NFE2 acts as a critical regulator of globin gene expression. NFE2 knockout mice feature a major defect in megakaryocyte biogenesis and severely impaired platelet production, whereas an abnormal increase in NFE2 expression is observed in hematological disorders such as polycythemias.[29] Recent studies shed light on various functional roles of NFE2 in nonhematopoietic tissues. Hepatic NFE2 overexpression has been found to promote gluconeogenesis

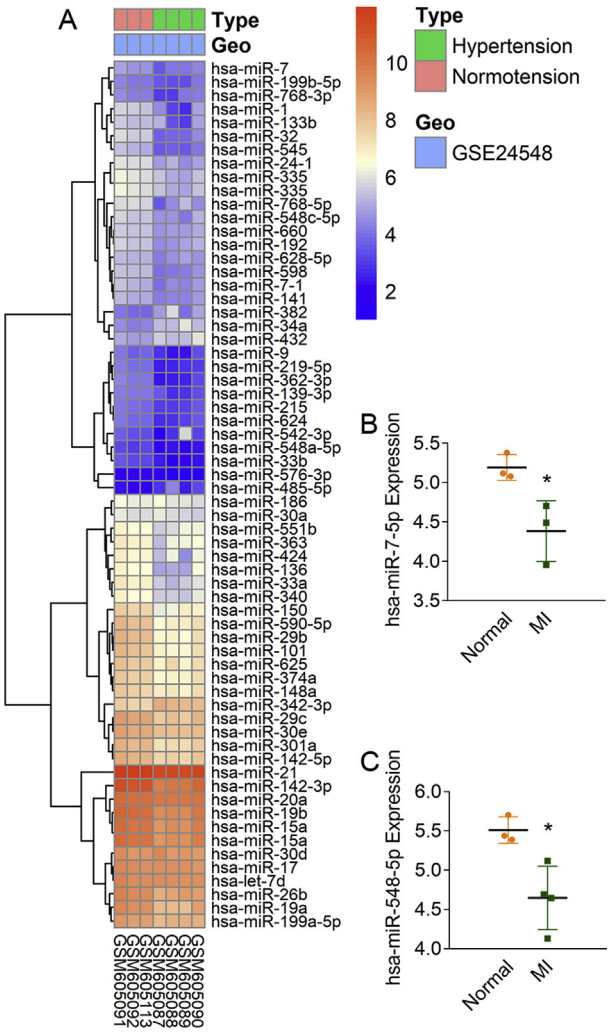

Figure 7 Hierarchical clustering analysis of DE-miRNAs. **(A)** Results of hierarchical clustering analysis of expression of MI-specific DE-miRNAs. **(B-C)** Microarray expression levels of miR-7 and miR-538 in GSE24548 in detailed representation. Orange: higher expression, blue: lower expression.

and lipid deposition and to cause hyperglycemia in normal mice through the FAM3A-ATP-Akt pathway.[30] The NFE2 transcription factor was identified more than 25 years ago, yet its roles in HT and myocardial tissues remain unclear. In this study, our dataset analysis revealed that this positive relation warrants further research on a direct link between FOLR3 or NFE2 and HT or MI. Notably, in patients with MI, GSEA showed higher levels of FOLR3 and NFE2 accompanied by an increasing expression of autophagy-related genes and a decreasing level of energy metabolism-related genes such as genes of the TCA cycle. This mechanism is similar to the compensatory increase in BNP levels in response to the relief of heart failure symptoms. Additional observational research should be conducted.

MiRNAs are well-known powerful regulators of gene expression. Their potential to serve as circulating biomarkers and for gene therapy with delivery by an adenovirus, plasmid, or lentiviral vector is widely accepted in terms of HT and MI.[31,32] By identifying the genes in the overlap between the set of predicted miRNAs targeting the co-DEGs and the set of DE-miRNAs specific to patients with MI, we found that miR-7 and miR-548 may be potential miRNA markers of HT-related MI. Previous research has confirmed that miR-7 and miR-26b are upregulated in the serum of HT patients with left ventricular hypertrophy, whereas miR-375, miR-7, and miR-29b expression is significantly altered in patients with primary aldosteronism, a common cause of human HT.[33,34] *In vitro* overexpression of miR-7b inhibits ischemia/reperfusion-induced apoptosis of H9C2 neonatal rat cardiac cells by targeting the HIF1a/p-P38 pathway.[35] On the other hand, IFN-λ1 (also known as IL-29), predicted and validated as the direct target of miR-548, is a major cytokine recently proven to suppress the migratory capacity of neutrophils and the formation neutrophil extracellular traps (NETs), which are a major mediator of thromboinflammation.[36,37] Polyphosphate released from activated platelets results in NET formation in patients with ST-segment elevation MI via mTOR inhibition and autophagy induction; these 2 pathways can be counteracted by IL-29 treatment, inhibiting NET formation.[38] At this point, our biological-category enrichment analysis gave rise to reasonable speculation about the cause of changes after MI with a complete closed loop. Decreased expression of miR-548 may upregulate 2 cardioprotective target genes (*FOLR3* and *IL-29* mRNAs), thereby reducing blood pressure and thrombus burden. This phenomenon may explain the enrichment results that we obtained regarding inflammation, immune-system-related biological processes, the TCA cycle, folic acid metabolism-associated molecular function, and abnormalities in such pathways as autophagy and the mTOR cascade.

Here, we suggest a new set of novel biomarkers and important molecular targets during the progression of HT and MI, including 2 co-DEGs (*FOLR3* and *NFE2* mRNAs) and 2 miRNAs (miR-7 and miR-548). This is the first data-mining study to identify co-expressed differentially expressed genes (co-DEGs) between HT and MI. Our biological-category enrichment analysis gave rise to reasonable speculation about the cause of changes after MI with a complete closed loop. Decreased expression of miR-548 may upregulate 2 cardioprotective target genes (FOLR3 and IL-29 mRNAs), thereby reducing blood pressure and thrombus burden.

PCR and ELISA may validate these markers for assessing the risk of HT-related MI. Experiments with *in vitro* and *in vivo* models as well as prospective clinical studies will be indispensable for validation of these markers for diagnosis and theragnostic.

Materials and methods

Microarray data and preprocessing

mRNA expression profiles (datasets GSE24752, GSE60993, and GSE62646) and an miRNA expression profile (the GSE24548 dataset) were retrieved from the Gene Expression Omnibus (GEO) database (https://www.ncbi.nlm.nih.gov/)[39] and were based on platform GPL570 (Affymetrix Human Genome U133 Plus 2.0 Array, Affymetrix Inc., Santa Clara, CA, USA), GPL6884 (Illumina HumanWG-6 v3.

0 Expression Beadchip, Illumina Inc., San Diego, CA, USA), GPL6244 (Affymetrix Human Gene 1.0 ST Array, Affymetrix Inc.), and GPL8227 (Agilent-019,118 Human miRNA Microarray 2.0 G4470B, Agilent Technologies, Palo Alto, CA, USA). Additionally, GSE24752 contains data on peripheral-blood samples from 3 patients with HT and 3 normotensive controls. The expression profiles of 17 blood samples (from patients with acute coronary syndrome visiting an emergency department within 4 h) and of 7 blood samples (from normal controls included in the GSE60993 dataset) were used to identify AMI-related gene expression differences and to determine enrichment with biological categories, together with 28 peripheral blood mononuclear cell samples from patients with ST-segment elevation MI on admission and 14 samples from patients with stable coronary artery disease without a history of MI as a control group included in the GSE62646 dataset, as complementary data processing. On the basis of the results, miRNA expression profiling data on platelets from 4 patients with very first acute MI and from 3 controls included in GSE24548 were selected for subsequent analysis of mRNA–miRNA regulatory networks.

Screening of DEGs

To assess and transform raw datasets, Perl software (Version 5.28.2) and R packages "affy," "limma," and "sva" were applied to conduct $\log_2$ transformation and background correlation.[40] Datasets GSE60993 and GSE62646 were combined by batch correction to eliminate the variance due to the interexperiment differences caused by subjective and objective factors, for more accurate and reliable results. Original P values were adjusted by the Benjamini–Hochberg method. However, the lowest P value (0.000123) was greater than the inverse of the total gene number (0.0001205) in GSE24752, meaning that the adjusted P values were unreliable. Because alterations of RNA levels are usually lower in peripheral-blood samples and peripheral blood mononuclear cells than in other tissues,[41] we used the criteria $|\log_2 FC| > 1$ (where FC is fold change) and original $P < 0.05$ to normalize the results and identify the DEGs in all the mRNA and miRNA datasets. Co-DEGs for HT-DEGs and MI-DEGs were identified in the overlap between these 2 gene sets in a Venn diagram.

Construction of interaction networks and functional enrichment

The Database for Annotation Visualization and Integrated Discovery (DAVID, https://david.ncifcrf.gov/) online database was utilized to annotate and visualize Gene Ontology (GO) enrichment using R package "GOplot." Kyoto Encyclopedia of Genes and Genomes (KEGG) pathway and REACTOME enrichment analyses were conducted and visualized using R packages "clusterProfiler" and "ReactomePA".[42,43] A *P* value cutoff <0.05 was assumed to indicate significant enrichment of co-DEG sets. To probe the potential pathways with respect to the cardiovascular effect of co-DEGs at the single-gene level, GSEA 3.0 (http://software.broadinstitute.org/gsea/index.jsp) software was used to analyze the combined dataset of GSE60993 and GSE62646, which is the transcription profile adjusted via array analysis of patients with MI according to a standard protocol.[44,45] DEG-encoded proteins were identified, and protein–protein interaction (PPI) network data were obtained using the Search Tool for the Retrieval of Interacting Genes database (STRING, http://string-db.org). The Cytoscape software (Version 3.6.1) was employed for the visualization of intranode connectivity degrees and interactions (or edges) among the candidate DEGs, with the following inclusion criterion: confidence score >0.4.

Identification and verification of miRNAs targeting DEGs

Online target prediction software microRNA Data Integration Portal (mirDIP, http://ophid.utoro nto.ca/mirDIP), TargetScan (version 7.1, http://www.targetscan.org/vert_71/), and miRWalk (http://mirwalk.umm.uni-heidelberg.de/) were used in combination to predict miRNAs targeting the co-DEGs. We selected top 5 candidate miRNAs of each co-DEG according to a higher prediction score from 2 or more prediction tools. The most representative and valuable predicted miRNAs for the co-DEGs as well as the DE-miRNAs from GSE24548 were studied via a Venn diagram to determine the overlap between the two gene sets.

Identification of genes associated with CVDs or metabolic diseases

The Rat Genome Database (RGD) Disease database (http://rgd.mcw.edu/wg/portals/) was utilized to determine the integrated gene landscape and enrichment with biological categories for *Homo sapiens* HT or MI. The Comparative Toxicogenomics Database (http://ctdbase.org/) was employed to predict novel associations between co-DEGs and CVDs or metabolic diseases via a computational prediction score.

Availability of data and material

The microarray datasets GSE60993, GSE62646, GSE24752, and GSE24548 can be obtained from the NCBI-GEO online database (https://www.ncbi.nlm.nih.gov/geo/query/acc.cgi).

Authors contribution

Wei Z.L. designed the study and performed the bioinformatics analysis. Wei Z.L., Li Q.L., and Yin Y. wrote this manuscript. Wei Z.H. and Xu B. were in charge of language editing. All the coauthors read and approved the final manuscript.

Conflict of Interests

The authors declare no conflict of interests.

Funding

This work was supported by the Postgraduate Research & Practice Innovation Program of Jiangsu Province (grant number KYCX18_1462), Nanjing Health Youth Talent Training Project in in 13th Five-Year (grant number QRX17113), Nanjing Medical Science and technique Development Foundation (grant number QRX17057) and the Natural Science Foundation of China (grant numbers 81700392 and 81601539).

Acknowledgements

The authors would like to thank the researchers who have uploaded their data to the databases employed in the present study.

List of abbreviations

HT	hypertension
AMI	acute myocardial infarction
ACS	acute coronary syndrome
CVD	cardiovascular diseases
GEO	Gene Expression Omnibus
KEGG	Kyoto Encyclopedia of Genes and Genomes
DAVID	The Database for Annotation Visualization and Integrated Discovery
STRING	Search Tool for the Retrieval of Interacting Genes database
DEG	differentially expressed gene
CO-DEG	co-expressed differentially expressed genes
GO	Gene Ontology
RGD	The Rat Genome Database
I/R	ischemia/reperfusion
PCI	percutaneous coronary intervention
SBP	systolic blood pressure
DBP	diastolic blood pressure
MACE	major adverse cardiovascular events
GSEA	Gene Set Enrichment Analysis
mirDIP	microRNA Data Integration Portal
CICH	cold-induced cardiac hypertrophy
FOLR3	folate receptor 3
NFE2	nuclear factor, erythroid-derived 2

References

1. Mozaffarian D, Benjamin EJ, Go AS, et al. Heart disease and stroke statistics-2015 update: a report from the American Heart Association. *Circulation*. 2015;131(4), e29-322.
2. Stephan D, Gaertner S, Cordeanu EM. A critical appraisal of the guidelines from France, the UK, Europe and the USA for the management of hypertension in adults. *Arch Cardiovasc Dis*. 2015;108(8—9):453—459.
3. Vasan RS, Beiser A, Seshadri S, et al. Residual lifetime risk for developing hypertension in middle-aged women and men: the Framingham Heart Study. *JAMA*. 2002;287(8):1003—1010.
4. Kearney PM, Whelton M, Reynolds K, Muntner P, Whelton PK, He J. Global burden of hypertension: analysis of worldwide data. *Lancet*. 2005;365(9455):217—223.
5. Diemer FS, Baldew SM, Haan YC, et al. Hypertension and cardiovascular risk profile in a middle-income setting: the HELISUR study. *Am J Hypertens*. 2017;30(11):1133—1140.
6. Robles NR, Macias JF. Hypertension in the elderly. *Cardiovasc Hematol Agents Med Chem*. 2015;12(3):136—145.
7. Bajaj A, Sethi A, Rathor P, Suppogu N, Sethi A. Acute complications of myocardial infarction in the current era: diagnosis and management. *J Invest Med*. 2015;63(7):844—855.
8. Prabhu SD, Frangogiannis NG. The biological basis for cardiac repair after myocardial infarction: from inflammation to fibrosis. *Circ Res*. 2016;119(1):91—112.
9. Ge Y, Wang TJ. Identifying novel biomarkers for cardiovascular disease risk prediction. *J Intern Med*. 2012;272(5):430—439.
10. Peymané A, Cheng KK, Jiang CQ, Zhang WS, Lam TH. Age-specific relevance of usual blood pressure to vascular mortality. *Lancet*. 2003;361(9366):1389—1390.
11. Levy D, Wilson PW, Anderson KM, Castelli WP. Stratifying the patient at risk from coronary disease: new insights from the Framingham Heart Study. *Am Heart J*. 1990;119(3 Pt 2): 712—717.
12. Park JS, Cha KS, Shin D, et al. Prognostic significance of presenting blood pressure in patients with ST-elevation myocardial infarction undergoing percutaneous coronary intervention. *Am J Hypertens*. 2015;28(6):797—805.
13. Pedrinelli R, Ballo P, Fiorentini C, et al. Hypertension and acute myocardial infarction: an overview. *J Cardiovasc Med (Hagerstown)*. 2012;13(3):194—202.
14. Liew CC, Ma J, Tang HC, Zheng R, Dempsey AA. The peripheral blood transcriptome dynamically reflects system wide biology: a potential diagnostic tool. *J Lab Clin Med*. 2006;147(3):126—132.
15. Shimoyama M, Laulederkind SJ, De Pons J, et al. Exploring human disease using the rat genome database. *Dis Mod Mech*. 2016;9(10):1089—1095.
16. Gao K, Shi X, Wang W. The life-course impact of smoking on hypertension, myocardial infarction and respiratory diseases. *Sci Rep*. 2017;7(1),e4330.
17. Isoyama S. Hypertension and age-related changes in the heart. Implications for drug therapy. *Drugs Aging*. 1994;5(2):102—115.
18. Bello Roufai M, Li H, Sun Z. Heart-specific inhibition of proto-oncogene c-myc attenuates cold-induced cardiac hypertrophy. *Gene Ther*. 2007;14(19):1406—1416.
19. Wang L, Yang B, Jiang H, et al. The molecular mechanism study of insulin in promoting wound healing under high-glucose conditions. *J Cell Biochem*. 2019;120(9):16244—16253.
20. Tydell CC, Yuan J, Tran P, Selsted ME. Bovine peptidoglycan recognition protein-S: antimicrobial activity, localization, secretion, and binding properties. *J Immunol (Baltimore, Md: 1950)*. 2006;176(2):1154—1162.
21. Park HJ, Noh JH, Eun JW, et al. Assessment and diagnostic relevance of novel serum biomarkers for early decision of ST-elevation myocardial infarction. *Oncotarget*. 2015;6(15): 12970—12983.
22. Mkaddem SB, Murua A, Flament H, et al. Lyn and Fyn function as molecular switches that control immunoreceptors to direct homeostasis or inflammation. *Nat Commun*. 2017;8(1),e246.
23. Delestre L, Cui H, Esposito M, et al. Senescence is a Spi1-induced anti-proliferative mechanism in primary hematopoietic cells. *Haematologica*. 2017;102(11):1850—1860.
24. Wagner B, da Silva Nardi F, Schramm S, et al. HLA-E allelic genotype correlates with HLA-E plasma levels and predicts early progression in chronic lymphocytic leukemia. *Cancer*. 2017;123(5):814—823.
25. Papandreou D, Malindretos P, Arvanitidou M, Makedou A, Rousso I. Homocysteine lowering with folic acid supplements in children: effects on blood pressure. *Int J Food Sci Nutr*. 2010; 61(1):11—17.
26. Palomba S, Falbo A, Giallauria F, et al. Effects of metformin with or without supplementation with folate on homocysteine

levels and vascular endothelium of women with polycystic ovary syndrome. *Diabetes Care*. 2010;33(2):246—251.
27. Evans RW, Shaten BJ, Hempel JD, Cutler JA, Kuller LH. Homocyst(e)ine and risk of cardiovascular disease in the multiple risk factor intervention trial. *Indian Heart J*. 2000;52(7 Suppl):S44—S52.
28. Veeranki S, Gandhapudi SK, Tyagi SC. Interactions of hyperhomocysteinemia and T cell immunity in causation of hypertension. *Can J Physiol Pharmacol*. 2017;95(3):239—246.
29. Gasiorek JJ, Blank V. Regulation and function of the NFE2 transcription factor in hematopoietic and non-hematopoietic cells. *Cell Mol Life Sci CMLS*. 2015;72(12):2323—2335.
30. Yang W, Wang J, Chen Z, et al. NFE2 induces miR-423-5p to promote gluconeogenesis and hyperglycemia by repressing the hepatic FAM3A-ATP-Akt pathway. *Diabetes*. 2017;66(7):1819—1832.
31. Schulte C, Karakas M, Zeller T. microRNAs in cardiovascular disease - clinical application. *Clin Chem Lab Med*. 2017;55(5):687—704.
32. Nemecz M, Alexandru N, Tanko G, Georgescu A. Role of MicroRNA in endothelial dysfunction and hypertension. *Curr Hypertens Rep*. 2016;18(12), e87.
33. Kaneto CM, Nascimento JS, Moreira MCR, et al. MicroRNA profiling identifies miR-7-5p and miR-26b-5p as differentially expressed in hypertensive patients with left ventricular hypertrophy. *Braz J Med Biol Res — Revista brasileira de pesquisas medicas e biologicas*. 2017;50(12), e6211.
34. He J, Cao Y, Su T, et al. Downregulation of miR-375 in aldosterone-producing adenomas promotes tumour cell growth via MTDH. *Clin Endocrinol*. 2015;83(4):581—589.
35. Sheng Z, Lu W, Zuo Z, et al. MicroRNA-7b attenuates ischemia/reperfusion-induced H9C2 cardiomyocyte apoptosis via the hypoxia inducible factor-1/p-p38 pathway. *J Cell Biochem*. 2019;120(6):9947—9955.
36. Xing TJ, Xu HT, Yu WQ, Wang B, Zhang J. MiRNA-548ah, a potential molecule associated with transition from immune tolerance to immune activation of chronic hepatitis B. *Int J Mol Sci*. 2014;15(8):14411—14426.
37. Cakmak Genc G, Dursun A, Karakas Celik S, Calik M, Kokturk F, Piskin IE. IL28B, IL29 and micro-RNA 548 in subacute sclerosing panencephalitis as a rare disease. *Gene*. 2018;678:73—78.
38. Chrysanthopoulou A, Kambas K, Stakos D, et al. Interferon lambda1/IL-29 and inorganic polyphosphate are novel regulators of neutrophil-driven thromboinflammation. *J Pathol*. 2017;243(1):111—122.
39. Barrett T, Wilhite SE, Ledoux P, et al. NCBI GEO: archive for functional genomics data sets-update. *Nucleic Acids Res*. 2013;41(Database issue):D991—D995.
40. Chen Z, McGee M, Liu Q, Scheuermann RH. A distribution free summarization method for Affymetrix GeneChip arrays. *Bioinformatics (Oxford, England)*. 2007;23(3):321—327.
41. Mohr S, Liew CC. The peripheral-blood transcriptome: new insights into disease and risk assessment. *Trends Mol Med*. 2007;13(10):422—432.
42. Yu G, Wang LG, Han Y, He QY. clusterProfiler: an R package for comparing biological themes among gene clusters. *Omics A J Integr Biol*. 2012;16(5):284—287.
43. Yu G, He QY. ReactomePA: an R/Bioconductor package for reactome pathway analysis and visualization. *Mol Biosyst*. 2016;12(2):477—479.
44. Subramanian A, Tamayo P, Mootha VK, et al. Gene set enrichment analysis: a knowledge-based approach for interpreting genome-wide expression profiles. *Proc Natl Acad Sci USA*. 2005;102(43):15545—15550.
45. Reimand J, Isserlin R, Voisin V, et al. Pathway enrichment analysis and visualization of omics data using g:Profiler, GSEA, Cytoscape and EnrichmentMap. *Nat Protoc*. 2019;14(2):482—517.